MSEG 624

Practical Electron Microscopy

Lab 2: SEM Imaging

Zachary Swain

Abstract

The effects of various operational parameters are examined for a JEOL JSM-7400F Scanning Electron Microscope. Detector geometry, probe current, working distance, and application of backscattered electron detection are varied to surmise their impact on SEM imaging. Here, their concluded effects are detailed and explained with reference to operational information of electron microscopy. This serves as a practical reference to aid in operation of a scanning electron microscope (SEM).

Performed on: March 14, 2019 Submitted on: March 29, 2019

Introduction

A scanning electron microscope operates by emitting a beam of electrons from a source, accelerating the beam down toward a specimen to be imaged, applying various operational parameters to the beam as it travels to the specimen, detecting subsequent electrons within the chamber, and converting that signal into a visual representation of the specimen. Different accelerating voltage, probe current, condenser, aperture, coil, lens, and working distance conditions can be applied in series, or parallel, to each other to reach a desired effect. In conjunction, they will dictate the features of the resulting specimen image. It is important to understand the operational parameters' impact on a resulting image in order to properly utilize this useful and important technology.

Experimental Methodology

In the experiments conducted, a magnesium oxide sample was imaged under various operating parameters of the JEOL JSM-7400F SEM. Images and corresponding imaging parameters were recorded under these varying conditions, and were later used to draw evaluations of contrasting and comparable aspects of each instance considered. The provided procedure entitled *EM Laboratory Exercise No. 1 & 2: SEM training and imaging*[1] was followed, with the exception of Section I – excluded at the discretion of laboratory Research Associate Dr. Zhao.

The sample was prepared for imaging beforehand, and placed into a sample holder. The sample was first placed into the sample exchange chamber, which was then closed and placed under a vacuum of 9.63E-5 Pa. After the vacuum had reached and stabilized at this value, the sample was then properly exchanged into the specimen

imaging chamber. The SEM was started and the sample was positioned for imaging and focused by utilizing Low Mag, Quick View, and ACB (automatic contrast and brightness) settings options.

Section II

To investigate the impact of detector geometry – first, an accelerating voltage of 3kV was used with a probe current of 8nA, at a working distance of 8mm. Imaging was conducted with the LEI secondary electron detector. The Wobble function was then executed and the X and Y knobs were used to minimize motion seen in the live image, aligning the objective aperture. Once the X and Y motion was minimized, leaving only a reciprocating focus, the Wobble function was stopped. The magnification was then set to 15,000x as an intermediary setting, and the image was focused at this magnification as to not lose track of focus set point once increased to a higher magnification. The magnification was increased to 60,000x (twice the desired setting), then focus, alignment, and X and Y stigmator were fine-adjusted to reduce effects of aberrations and for optimal imaging. Finally, the magnification was reduced to 30,000x, the image was adjusted by ACB, and an image was recorded.

Next, the detector being used was changed to the SEI in-lens detector. The magnification was again lowered to 15,000x and the image was wobbled and focused. The same feature that was imaged with the LEI detector was located and magnified to 60,000x. The image was focused and the X and Y stigmator were properly adjusted. The magnification was reduced to 30,000x and ACB was used to tune the image; an image was then recorded.

Section III

Next, altering the probe current was investigated to have effect on imaging. The 3kV accelerating voltage, 8nA probe current, and 8mm working distance were maintained from the previous experiment, but the detector was reverted to the LEI detector. The same feature was located as was imaged in Section II, and magnified to 15,000x. Wobble and focus were similarly adjusted, as before. The magnification was then increased to 100,000x, then the image focus and stigmator were fine adjusted for optimal imaging. The magnification was then decreased to 5,000x, ACB adjusted the image, and the image was recorded. A second image was recorded after increasing the magnification to 50,000x. This same process was then repeated to record 5,000x and 50,000x images of the same feature, but using a probe current of 15nA.

Section IV

To investigate the effect of working distance on imaging resolution, the probe current was reduced back to 8nA and the working distance was increased to 10mm; but the 3kV accelerating voltage and LEI detector remained unchanged, at first. The image was focused and stigmator adjusted for the new probe current and working distance conditions, then magnified to 100,000x on the same feature as before. It was refocused and the stigmator X and Y tuned for the new, increased magnification. The magnification was then decreased to 60,000x and ACB adjusted before imaging and recording the sample feature. These steps were then repeated after decreasing the working distance to 6mm, and an image was recorded at this decreased working distance.

Lastly, the working distance was decreased to 3 mm. For this small working distance, the detector was switched to SEI because the LEI detector is positioned at an angle relative to the sample stage in order to detect secondary electrons as they exit into the chamber. When the sample stage is so close, there are not sufficient secondary electrons that exit at an angle necessary to reach the LEI detector. The SEI does not have this issue, as it is an in-lens detector and will receive a normal amount of secondary electrons at this close working distance – producing a good signal. Once the SEI detector was selected, the image was wobbled for the new detector, and the image was focused and X and Y stigmator adjusted at 100,000x magnification, as before. The magnification was then decreased to 60,000x and ACB adjusted, then an image was recorded.

Section V

The next experiment focused on the impact of working distance on depth of field, specifically. The SEM was kept at 3kV accelerating voltage and 8nA probe current, but the detector was reverted to LEI and the working distance was set to 6mm. The magnification was reduced to 1,000x for this experiment. The wobble function was executed, and the aperture alignment was corrected for the new detector. The image was then optimized (focused and stigmator adjusted at higher magnification) for 1,000x magnification, and an image was recorded. The working distance was then increased to 15mm and the imaging parameters were again optimized, before recording an image at the higher working distance.

Section VI

The final experiment was to compare the image effects of utilizing a backscattered electron detector (BSD) to that of an in-lens secondary electron detector

(SEI). A different sample was used for this experiment, so the magnesium oxide sample was removed and a Ru/ɣ-Al_2O_3 sample was imaged instead. An accelerating voltage of 10kV and initial probe current of 10nA were selected to image the sample at a working distance of 6mm. The sample was first imaged using the SEI in-lens detector. The wobble, focus, and stigmate were optimized for 5,000x imaging (configured at higher magnification). The image was ACB adjusted and an image of the sample was recorded at 5,000x. The COMPO detector setting was selected and the BSD was inserted by a pneumatic valve mechanism within the microscope. The image was wobbled, focused and stigmate adjusted. The focus was deemed not to be ideal, and the probe current was increased to 11 nA, then reconfigured and imaged as prior.

Results and Discussion

In total, 13 images were obtained to characterize the impact of select operating parameters on image features. Secondary detector geometry, probe current, working distance (resolution, depth of field), and backscattered detector effects were each isolated comparatively. Here, their impact will be visualized in their imaging and discussed.

Section II

In the first experiment performed, the effect of secondary electron detector geometry was compared by using both LEI and SEI mode to image the same feature, with other parameters remaining unchanged. Fig. 1 shows the two images recorded in this experiment, and clearly displays some of the contrasting elements of both techniques.

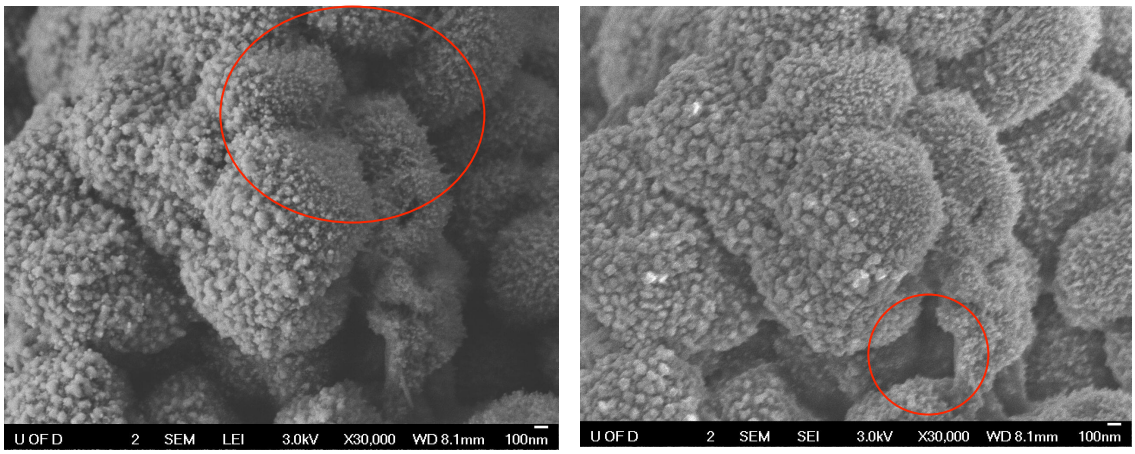

FIG. 1: MgO imaged at 30,000x using secondary electron detectors. Left: LEI detector is used to image. Right: SEI detector is used to image. Topological information and crevice detail respectively circled for comparison.

The LEI detector shows more shading and creates a more "three dimensional" image, displaying more topographical information, whereas the SEI detector provided a more evenly detailed image – both in the image plane and in the z-axis. While the LEI was able to convey more detail about each feature's relative height, the SEI provided greater detail in topological crevices, and on the side opposite the LEI. The result is a more complete in-plane image by the SEI detector, but more topology information from the LEI detector.

This effect is likely due to the detectors' respective placement within the chamber. The LEI is both above and off to the side of the sample, collecting secondary electrons exiting at an angle. The result is a constructed top-down view of the specimen, displaying topological information not detected from the beam axis. But since the SEI in-lens detector does image from the beam axis, it is able to provide more complete information of creviced features below the "line-of-sight" of the LEI detector. This provides better detail and illumination of features of lower relative height, respective to the image plane; whereas the SEI detector provides more detail about that relative height difference.

Section III

The investigation into how a difference in probe current may affect a sample image proved fruitful in its endeavor as well. Some clear disparities in image detail and aspects provided insight into how this imaging parameter can influence imaging of a specimen. Fig. 2 displays both the lower and higher magnification trials of the probe current experiment, and each depicts a unique aspect of its imaging conditions to be taken into account.

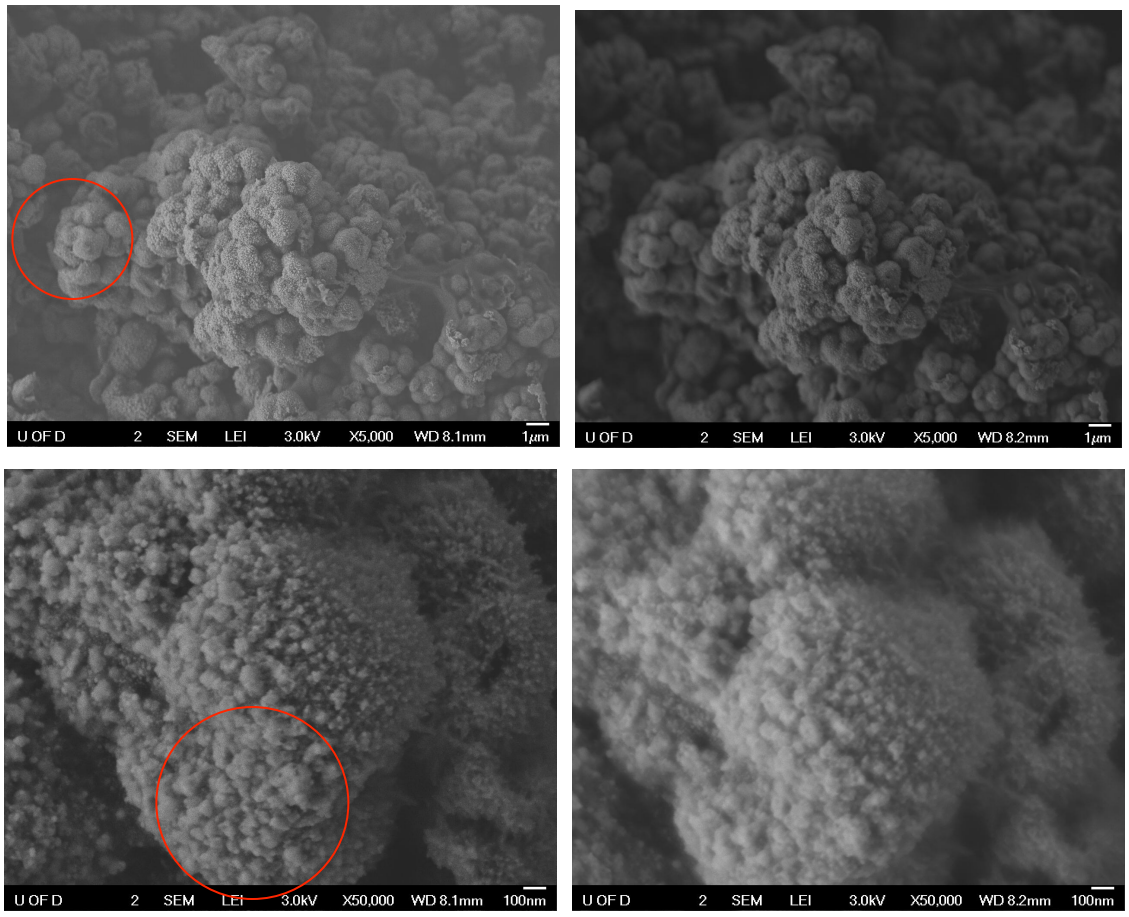

FIG. 2: MgO imaged using LEI detector. Top-left: 8nA current at 5,000x. Top-right: 15nA current at 5,000x. Bottom-left: 8nA current at 50,000x. Bottom-right: 15nA current at 50,000x. Depth of field and S/N differences at 5,000x and 50,000x, respectively, are circled for comparison.

The smaller probe current of 8nA proved to be more desirable at the 5,000x and 50,000x magnifications examined for both depth of field and feature resolution. A smaller probe current provides a smaller probe diameter, which gives greater resolution and a sharper image – whereas a larger probe current constructs an image with more surface smoothing.

A smaller probe current is likewise seen to increase the depth of field, as a smaller aperture does. From these observations, the 8nA probe current is the obvious choice for both magnifications, given the sample and conditions chosen here. A probe current of 15nA seems to be generally undesirable for LEI imaging, but may be useful for EDS imaging. Such a high probe current for LEI secondary electron imaging also leads to charging effects, which will likewise affect the signal-to-noise ratio (S/N). If charging effects are seen while imaging, a decrease in probe current and/or accelerating voltage should mitigate the charging to an extent – their respective physical impact being less electrons interacting with the specimen and/or the electrons travelling at a slower rate. Depending on the sample's material, it may be useful to sputter-coat the specimen with a thin layer of conductive Au or C to alleviate the charging effects.

Section IV

The variation of working distance (WD)examined in the third experiment conducted was seen to have an appreciable impact on image resolution. A smaller working distance will act to decrease beam spot size, and provide better image resolution. The effects of a working distance ranging from 3-10mm at a magnification of 60,000x are seen in Fig. 3. The10mm WD provides noticeably worse resolution that that of the 6mm WD, which in turn shows less detail than the 3mm WD.

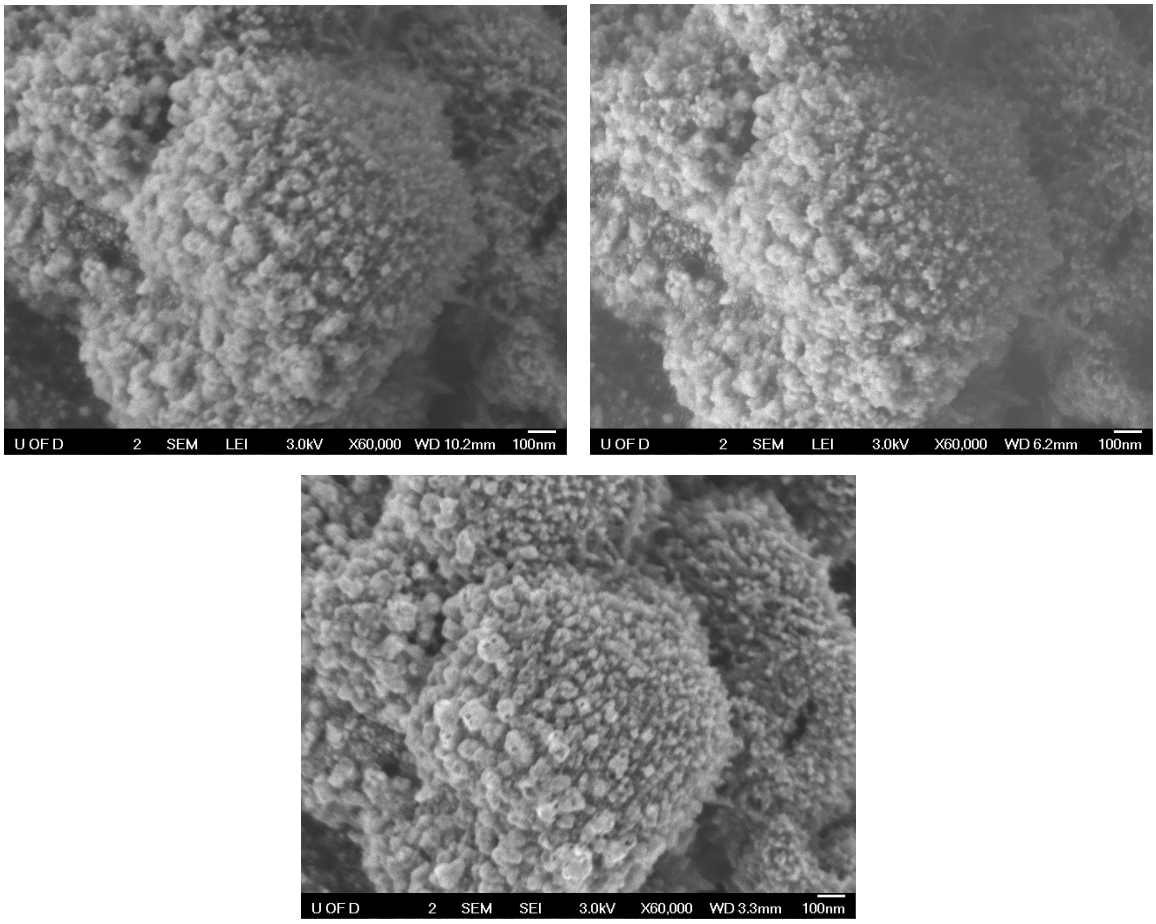

FIG. 3: MgO imaged at 60,000x using LEI and SEI detectors. Top-left: 10mm WD LEI. Top-right: 6mm WD LEI. Bottom: 3mm WD SEI.

Smaller features can be seen more clearly, and less obscured, in the 6mm WD than in the 10mm WD. As the SEI detector must be used for the 3mm working distance – as detailed in the provided experimental methodology – the disparity in image aspects of LEI and SEI imaging are further depicted in this experiment. It is important to note that there is some error in the WD setting when weighed against its measurement. When the sample is placed in the sample holder, it is "eyeballed" to be nearly flush with the top surface of the specimen holder, but not done so precisely. The inherent inaccuracy in estimating the z-axis positioning of the specimen gives rise to inaccuracy in set WD. This can be seen in the images above, having displayed WDs of 10.2, 6.2, and 3.3.

Section V

Working distance was also varied at lower magnification to gauge its effect on depth of field, and was seen to provide better depth of field when increased. This effect can be visualized in Fig. 4, displaying the images captured in the experiment.

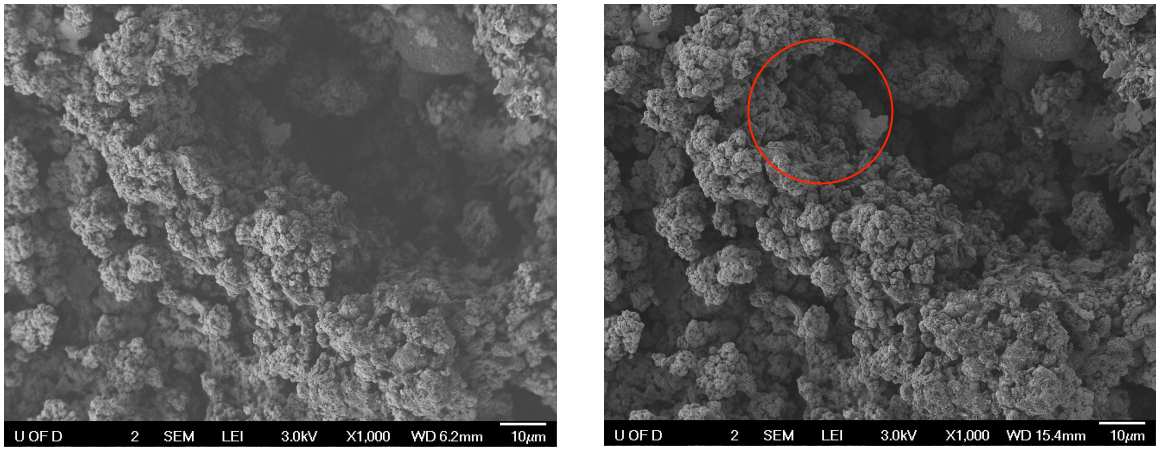

FIG. 4: MgO imaged at 1,000x using LEI detector. Left: 6mm WD. Right: 10mm WD. Feature of relative depth circled for comparison.

The image taken at 10mm WD can be seen to focus features of relative depth significantly better than the 6mm WD image. A larger working distance provides a larger spacing between the bottom surface of the objective lens and the top surface of the specimen. When properly focused on that top surface, the focal plane is further from the objective lens and thus has a lesser angle relative to the beam axis. This results in less deviation in focus over a set distance along the z-axis and provides a greater depth of focus, as a feature must be further from the objective lens to defocus by the same extent when compared to a smaller WD.

Section VI

The Ru/ɣ-Al_2O_3 specimen was found to image quite differently with the BSD, as compared to the SEI image. The resulting images of each detector configuration are shown below in Fig. 5 where the COMPO image displays contrasting composition, as compared to the SEI image.

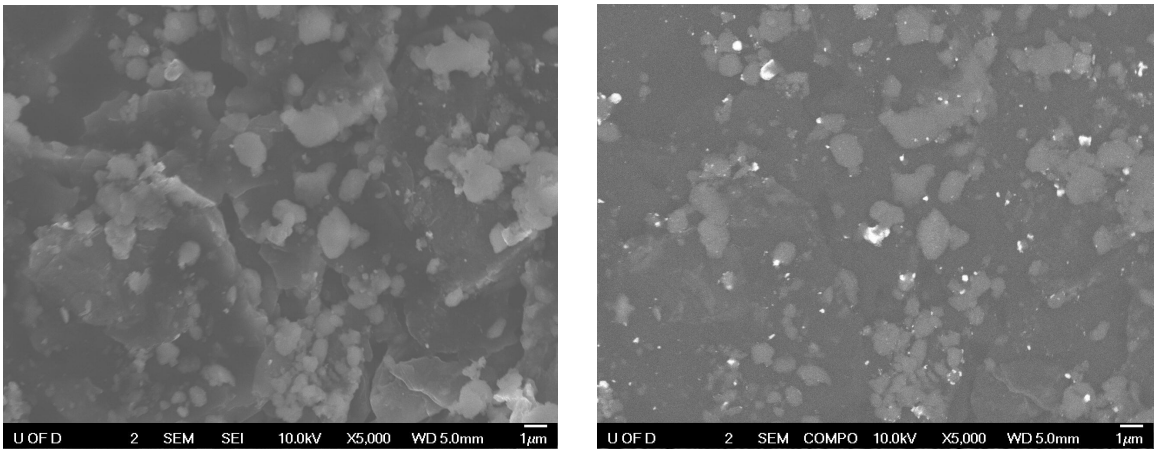

FIG. 5: Ru/ɣ-Al_2O_3 imaged at 5,000x using LEI and COMPO detector settings. Left: LEI. Right: COMPO

The BSD appears to illuminate locations on the specimen where the ruthenium is present, which is not readily apparent in the normal SEI image. The heavier element is more effective in backscattering electrons and produces a larger local backscattering signal, which is then detected by the BSD. This is useful for determining location and size uniformity of a specific sample composed of elements of contrasting density. It can also be used to approximate the composition percentage of a particular heavy element. University of Delaware Center for Composite Materials' SMARTree image analysis software suite[2] was used to estimate the in-plane compositional percentage of ruthenium, as displayed below in Fig. 6.

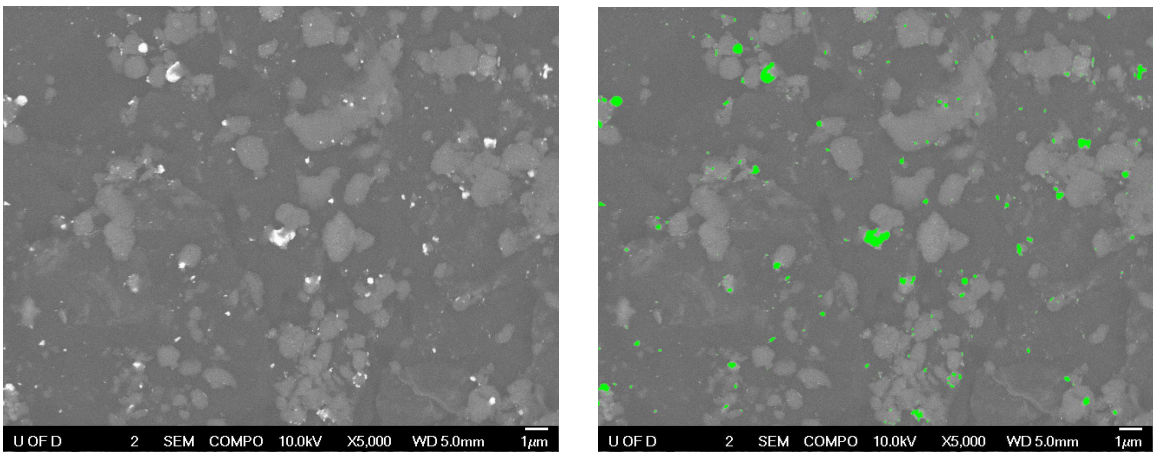

FIG. 6: Ru/ɣ-Al_2O_3 imaged at 5,000x with COMPO detector setting and then analyzed using SMARTree. Left: Resulting image of BSD, highlighting Ru pockets. Right: SMARTree analysis isolating Ru pockets (green).

The SMARTree image analysis resulted in a Ru content of 1.37%. This can be related to the entire sample, assuming that the interaction volume imaged in this trial is representative of bulk structure. If the ruthenium content can be reasonably estimated to not vary in-plane or at depths other than that imaged here, then the bulk structure this specimen was sampled from can be extrapolated to likewise contain about 1.37% Ru.

Summary

Through the experimentation detailed above, the conclusions are reached that LEI imaging provides better topographical information while SEI imaging results a more complete detailing of in-plane features. Increasing probe current to 15nA is found to result in worse resolution and depth of field. While resolution increases as working distance decreases, a larger working distance will provide a greater depth of field. And BSD imaging can be utilized to identify (and subsequently quantify) elemental mapping and estimate compositional percentage.

Acknowledgements

Thank you to Dr. Ni and Dr. Zhao for teaching me this material and providing lab space in which to conduct these experiments.

References

[1] Ni, Chaoying, "*EM Laboratory Exercise No. 1 & 2: SEM training and imaging*," MSEG624 Practical Electron Microscopy, University of Delaware, Spring 2019.

[2] SMARTree Software https://gitlab.ccm.udel.edu/SMARTree

Supplemental

All files used and supplementary material can be found at:

https://github.com/zswain/MSEG624